

## **Studies on Au colloid-embedded active-carbon based supercapacitors: the case for a plasmonics effect at the Electrolyte/Electrode Interface**

H. Grebel<sup>(1)</sup> and Yuanwei Zhang<sup>(2)</sup>

<sup>(1)</sup> Center for Energy Efficiency, Resilience and Innovation (CEERI) and the ECE Department at the New Jersey Institute of Technology, Newark, NJ 07102. [grebel@njit.edu](mailto:grebel@njit.edu)

<sup>(2)</sup> Department of Chemistry and Environmental Science at the New Jersey Institute of Technology, Newark, NJ 07102. [yuanwei.zhang@njit.edu](mailto:yuanwei.zhang@njit.edu)

### **Abstract**

Supercapacitors (S-C) are fast charge/discharge elements. These short-term energy storage found many applications; among which is mitigation of the impact that highly fluctuating sustainable sources have on power grids. For double-layer S-C, one takes advantage of the very narrow interface between an electrolyte and a conductive porous electrode. In contrast, ordinary capacitors are made of a relatively thicker dielectric material, sandwiched between two electrodes. In the past, polarity increase was achieved by dispersing conductive colloids in the dielectric material. Used primarily for microwave and optical devices – a field known as plasmonics - its impact on the low frequency supercapacitor is unknown. Here we explore the addition of nano-size Au particles (AuNP) to active-carbon electrodes to find a large specific capacitance increase.

## I. Introduction

Originally devised for microwave lenses, Artificial Dielectrics (AD) are man-made materials that contain metal particles much smaller than a characteristic propagating wavelength (e.g., mm-size ball bearings at a wavelength of 3 cm) [1-3]. These features alter the effective permittivity and permeability of the dielectric through creation of locally induced dipoles. Dipole-dipole interaction should be considered at large dispersions. Stained glasses, which exhibit bright colors when nano-size gold or, silver colloids are embedded in them are yet another example. Finally, the enhancement of the electric field at the vicinity of metal colloids is used to amplify molecular Raman signals (Surface Enhanced Raman Scattering, SERS). This concept was extended to include nano-size semiconductor embedded dielectrics [4,5] when realizing light-controlled devices (aka Conditional AD, or CAD). While there is a large body of work on AD at the high-frequency region, little if at all, has been investigated at the low frequency end, and in particular, in the range of Hz or kHz.

Supercapacitors, S-C, [6-11] are capacitors that take advantage of the large capacitance at the interface between an electrode and an electrolyte. Here, we concentrate on carbon based S-C that exhibit electrical double-layer behavior. S-C have found many energy applications due to their fast charging and discharging. These include, mitigation of highly fluctuating micro-grids [12-13], or optical modulators [14]. Our intent is to gain basic knowledge on the capacitance changes when incorporating very low concentration of gold colloids in active carbon (A-C) based electrodes. On one hand, the capacitance of S-C occurs within a very narrow region of nanometer range at the electrolyte/electrode interface and at concentration levels of  $\mu\text{g/mL}$ , the effect if exists, should be minimal. On the other hand, if the gold colloids are placed within the double-layer region of the electrolytic capacitor, then one expects a large polarization effect, similarly to AD materials.

Dispersions of Au nano-particles (AuNP) have been known for a long time [15]. In order to ensure a good suspension, the colloids are coated with a ligand that is negatively charged. The charged surface enhances the electrostatic bond between the neutral, yet conductive A-C electrode and the AuNP. The suspension in water exhibits red-wine color for ca 50 nm particles, bluish color for ca <100 nm particles and purplish/brown color for larger size colloids [16]. The larger size colloids of >100 nm tend to aggregate and exhibit sedimentation. Here, data on two colloidal sizes, various polymeric binders and various electrolytes exhibit an enhanced specific capacitance when the AuNP are incorporated in A-C based S-C.

## II. Materials and Methods

### Preparation methods: gold colloids

Nano-size AuNPs were synthesized following literature method using citrate as a reducing agent and stabilizer [17]. In brief, chloroauric acid ( $\text{HAuCl}_4$ ) water solution (10 mg  $\text{HAuCl}_4$  in 90 ml of water) was heated to boiling and sodium citrate solution (0.5 ml of 250 mM) was introduced. The mixture was stirred for 30 min until the color turned to wine red. AuNPs were then purified by centrifuge and washed with DI water three times.

There were 2 batches of suspended AuNP in water: medium size exhibiting blue/wine color, Figs. 3-7) whose light absorption data is shown in Fig. 1 and an aggregated batch (~100 nm Fig. 9) exhibiting sedimentation.

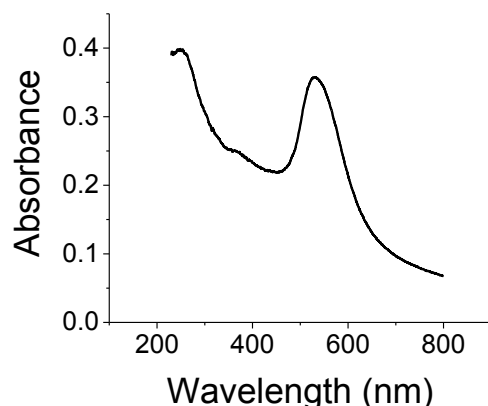


Figure. 1. Absorbance data for the smaller size AuNPs, suspended in water. DLS data indicates an averaged size of 45 nm.

### Preparation methods: porous electrodes

(a1) A single batch of active-carbon (A-C) with a 5% Cellulose Acetate Butyrate (CAB) binder was prepared. The 20 mL of acetone contained 2 gr of A-C and 100 mg of CAB. Six samples, each containing 1 mL of the slurry were prepared. To these, succession amounts of 10  $\mu$ L of AuNP, suspended in water were added. Each mixture was first sonicated with a horn antenna, dropped casted on grafoil electrodes (area of contact 1.27x1.27 cm<sup>2</sup>, or 0.5"x0.5 inch<sup>2</sup>), baked on a hot plate at <90°C and then soaked with an electrolyte (1 M of Na<sub>2</sub>SO<sub>4</sub>, or NaCl). A fiberglass filter (Whatmen 1851-055) was used as a membrane. The Au colloid concentration was 1 mg/mL. The pores in the A-C electrodes are of the order of sub-microns [18-19].

(a2) Variation on (a1) includes the suspension of A-C and AuNP in acetone, sonication, addition of dissolved CAB in 1 mL acetone, sonication and drop casting.

(b) Similar to (a) but with Poly-Vinyl Alcohol (PVA) as a binder and 1 M of NaCl as an electrolyte. The Au colloids sizes were of order of >100 nm, exhibited some sedimentation and deemed as aggregates per their purplish/bluish color that tended to brown. Their concentration was 1 mg/mL.

**The samples:** Cuts of 200 micron thick grafoil electrodes with back adhesive (1.27 cm x 2.54 cm) were placed on similar cut microscope slides. Before placing it on the slides, the grafoil electrodes were placed in 1 M NaOH container and were exposed for 30 sec to microwave radiation in a microwave oven to improve adhesion of the binder to the grafoil. The two slides were held by tweezers (or clips) and the boundaries of the sample were left unsealed while soaking it in the electrolyte. The sample configuration is shown in Fig. 2a and its picture in Fig.2b.



Figure 2. (a) A cross section of sample with grafoil coated active-carbon (A-C) electrodes, and (b) a picture of the cover area ca, 12.7x12.7 mm<sup>2</sup>.

### Electrochemical Techniques:

Potentiostat/Galvanostat (Metrohm) was used. Each sample was tested using three electrochemical methods: Cyclic Voltammetry (C-V), Charge-Discharge (C-D) and Electrochemical Impedance Spectroscopy (EIS). These methods all agreed on the titration trend.

### Initial Characterizations:

By itself, un-coated grafoil electrodes exhibited very small capacitance values (Fig. 3a). Thicker grafoil electrodes exhibited an inferior capacitance to the thinner ones, probably due to manufacturing differences. Electrochemical Impedance Spectroscopy (EIS) (Fig. 3b) reveals that there little change in the differential capacitance as a function of light when the A-C films were placed on ITO electrodes and subjected to irradiation by a 75 W of light, similarly to past experiments on semiconductive particles [18-19]. There is relatively large change of the electrode resistance (up to the knee of the curve). A light induced increase in the cell polarization is observed around the curve's knee indicating reduction in ion diffusion [20]. Overall, the optical effect is small (~6%) and is attributed to optical excitation in both the A-C and the ITO electrode.

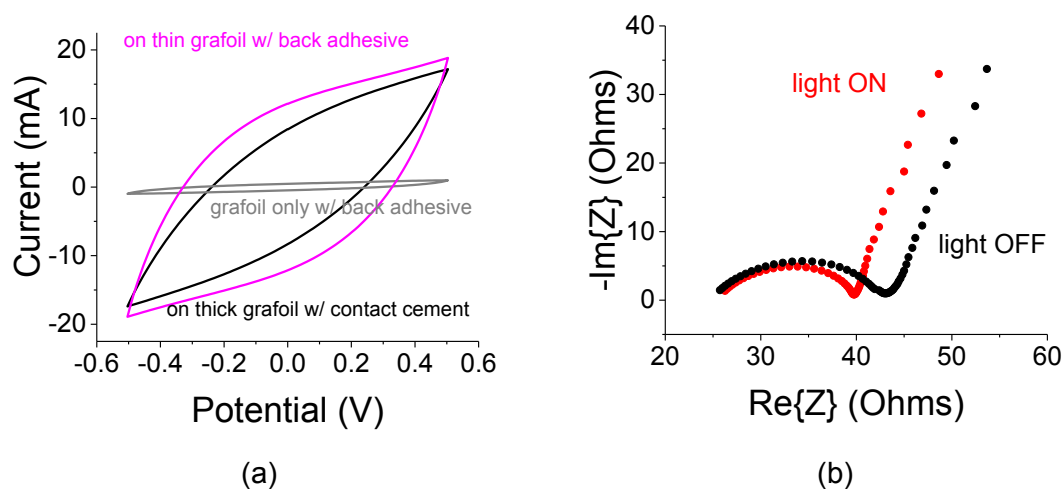


Figure 3. (a) Initial C-V traces for A-C deposited (pink and black curves) and uncoated (grey curve) on various grafoil based current collectors; thick and thin electrodes refer to thickness values of 500 and 200 micron, respectively. (b) EIS curves under 75 W white light for colloidal embedded sample on ITO substrate (instead of the grafoil electrodes).

Titration experiments have been carried out. The initial idea was that larger AuNP concentration will lend itself to larger capacitance values as more colloids will find itself at the electrolyte/electrode interface. Initial C-V experiments with 1 M of  $\text{Na}_2\text{SO}_4$  were made as indicated by Fig. 4a. These experiments exhibited a capacitance peak at AuNP concentration of 40  $\mu\text{g}/\text{mL}$ . The related capacitances as a function of AuNP concentration are shown in Fig. 4b. Note a capacitance increase by a factor of ~2 as a result of AuNP presence when compared to a reference sample without them. Since the amount of active carbon in each vial was 100 mg/mL, the concentration of the gold colloid with respect to that of the A-C is written as  $\mu\text{g}/100 \text{ mg}$ . The amount of gold is very small in comparison to the amount of A-C, and as suggested below this large effect could be more to do with the placement of the colloids rather than with their increased concentration.

The area of each sample is the same and the related capacitance values of Fig. 4a may be viewed as specific areal capacitance. For examples, the peak capacitance of 110 mF at 40  $\mu\text{g}/100\text{ mg}$  is translated to  $110\text{ mF}/1.27^2\text{ cm}^2=68.2\text{ mF}/\text{cm}^2$ . The trend in Fig. 4 is also exhibited in Fig. 5a,b and Fig. 6a,b for C-D and EIS experiments, respectively.

Two reference experiments were additionally made: (1) a repeat of the 50  $\mu\text{L}$  experiment on another grafoil substrate to assess variations in sample preparation. That variation was estimated at  $\pm 5\%$ . (2) 30  $\mu\text{L}$  of AuNP were added to the mixture holding 30  $\mu\text{L}$  of AuNP (in total 60  $\mu\text{L}$  of AUNP in 1 mL) to assess an increase in colloid concentration. 'Mix and match' experiments are detailed in Fig. S1 in the Supplemental Information Section.

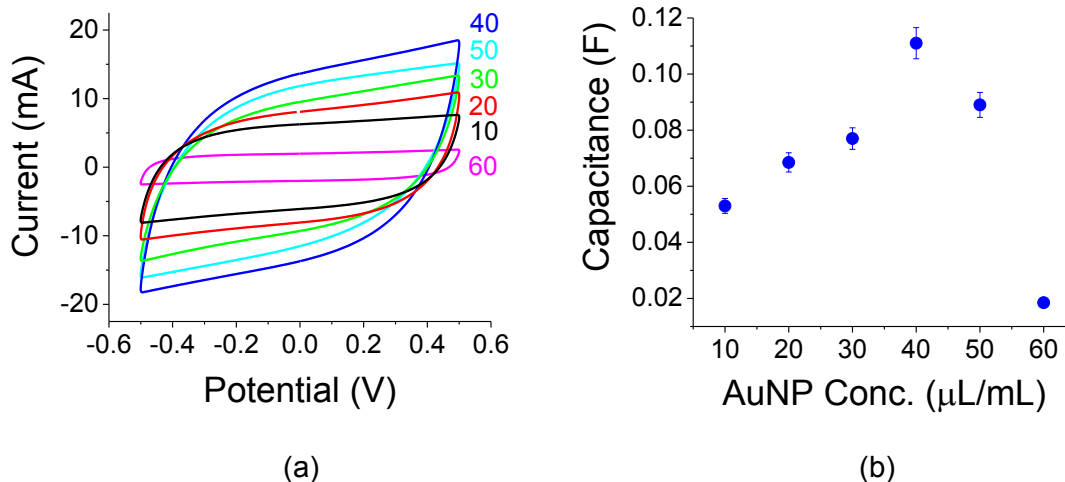


Figure 4. (a) Successive C-V plots for various concentrations (micro-L/mL) depicted on the right. (b) Capacitance as a function of AuNP concentration exhibits a peak at 40  $\mu\text{L}/\text{mL}$ . The electrolyte was 1 M of  $\text{Na}_2\text{SO}_4$ .

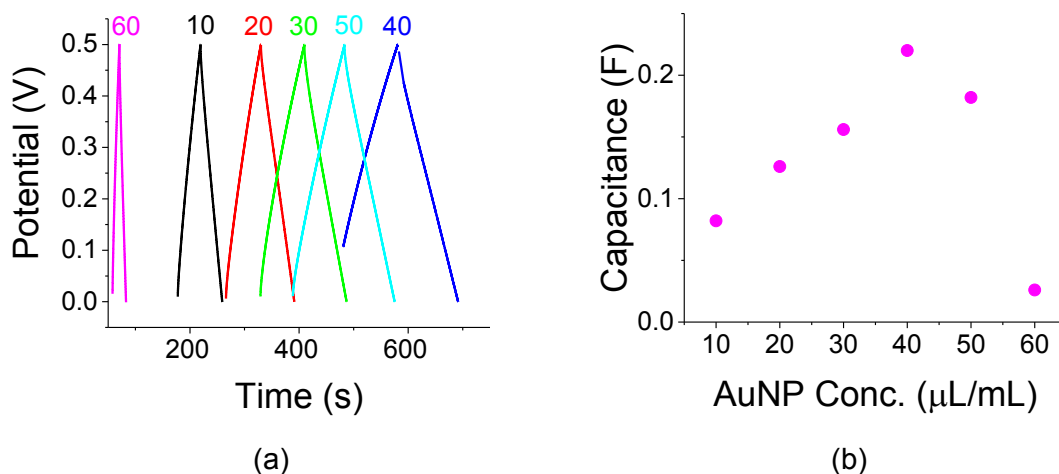


Figure 5. (a) C-D plots for various AuNP concentration (in  $\mu\text{L}/\text{mL}$ ). (b) Capacitance as a function of AuNP concentration exhibits a peak at 40  $\mu\text{L}/\text{mL}$ . The electrolyte was 1 M of  $\text{Na}_2\text{SO}_4$ .

Finally, Electrochemical Impedance Spectroscopy (EIS) for the maximum capacitance is shown in Fig. 6a. The slope of the curve in Fig. 6b is proportional to the inverse of the differential capacitance,  $C_{diff}$ , as,  $1/(2\pi C_{diff})$  [20].  $C_{diff}$  may be calculated as 0.194 F, corroborating the value obtained from Fig. 2b. Overall, the electrode resistance (ca 3-5 Ohms for all samples) is rather small.

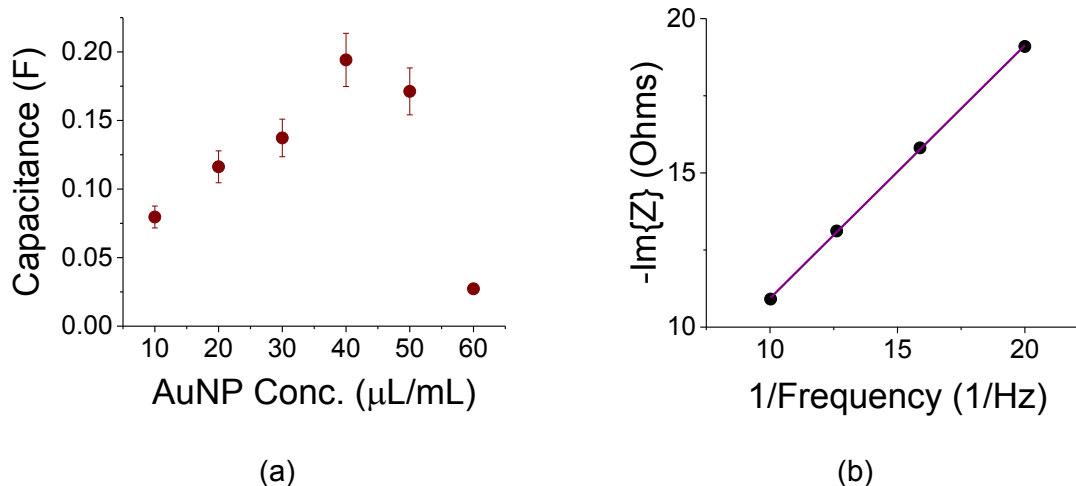


Figure 6. (a) Capacitance values, derived from EIS curves. (b) The slope of the linear curve for the sample exhibiting capacitance maxima at 40  $\mu\text{L/mL}$  of AuNP is proportional to  $1/C_{diff}$ . The electrolyte was 1 M of  $\text{Na}_2\text{SO}_4$ .

One could argue that values of film capacitance, or even values of specific capacitance with respect to the area (in units of  $[\text{F}/\text{cm}^2]$ ), do not provide for a full picture because the electrolyte may penetrate through the polymeric binder and probe the entire film thickness [21]. Plots of the specific gravitonic capacitance in units of  $\text{F/g}$  were made for different set of films at various conditions (various thicknesses, binders and electrolytes) as outlined below.

We note that the area of the sample is the same,  $1.61 \text{ cm}^2$ . The density of the composite film,  $d_{film}$ , is a weighted density of its components: 95% of A-C and 5% of polymeric binder which are kept the same throughout all tests:  $d_{film} = 0.95 \times (d_{A-C} = 0.375 \text{ g/cm}^3) + 0.05 \times (d_{polymer} = 1.21 \text{ g/cm}^3) \sim 0.42 \text{ g/cm}^3$ . The volume is  $A \times t$  and the film thickness is  $t = w_{film} / (d_{film} \times A)$  with  $w_{film}$  being the film weight. The gravitonic specific capacitance in units of  $\text{F/g}$  is related to the volumetric specific capacitance in units of  $[\text{F}/\text{cm}^3]$  as:  $[\text{F}/\text{cm}^3] = [\text{F} \times (\text{g}/\text{cm}^3) / \text{g}] = [\text{F} \times d_{film} / \text{g}]$ . Therefore, gravitonic and volumetric specific capacitance values are proportional to one another by a constant: the film density of  $d_{film} = 0.42 \text{ g/cm}^3$ .

### III. Results

Two sets of experiments were carried out: one for thicker ( $\sim 450 \mu\text{m}$ ) and the other for thinner ( $\sim 75 \mu\text{m}$ ) films. Their results are shown in Fig. 7. The thin films were obtained by further dilution of the original batches by 1 + 1 mL of acetone + ethanol for a total of 3 mL solution. The concentration of the AuNP is referenced to the amount of the A-C in the sample because both the AuNP and the A-C were diluted by the same amount. The trend exhibited by the thicker and thinner films is the same; thinner films exhibited larger specific values [22]. The consistent results for the reference sample (0  $\mu\text{g}/100 \text{ mg}$ ) alludes to the repeatability of the experiments. Of interest are the relatively large values at 20 and 50  $\mu\text{g}/100 \text{ mg}$ . As also suggested by Fig. 9, the large variability of values at 50  $\mu\text{g}/100 \text{ mg}$  in Fig. 7 may be attributed to lower film integrity due to a

mixture of hydrophobic and hydrophilic components; the AuNPs are suspended in water while the A-C and the CAB binder are hydrophobic.

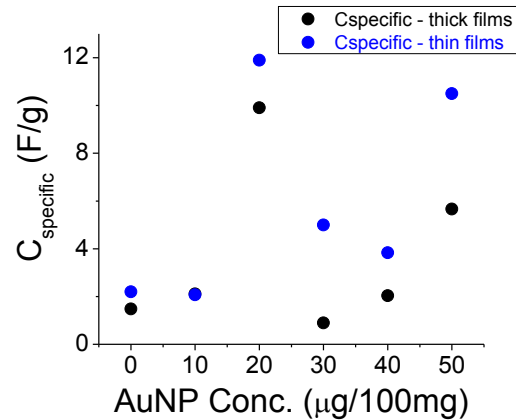


Figure 7. Specific capacitance,  $C_{\text{specific}}$  in units of F/g from C-V data for thick and thin films with a CAB binder. The electrolyte was 1 M of  $\text{Na}_2\text{SO}_4$ .

Another set of tests was conducted with the smaller size AuNP colloids (~45 nm of Fig. 1), yet with 1 M NaCl as an electrolyte. Better film homogeneity was achieved by first sonicating the AuNP with A-C in 1 mL of acetone following with 1 mL of 6% CAB by weight in acetone, as well; the latter mixture was re-sonicated. The results shown in Fig. 8 are consistent with the previous results. The peak value seem to shift a bit towards a larger concentration.

We found out that incorporating the AuNP in the electrolyte did not yield any capacitance increase. This is probably due to screening by the ions in the electrolyte. Administrating the AuNP in polymeric binder before adding the A-C was also not efficient. Adding the AuNP to a thin polymeric layer directly on the grafoil film resulted in a very poor capacitor because it blocked the collection of current.

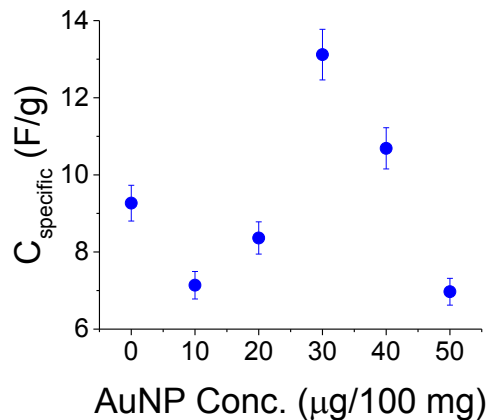


Figure 8. Specific capacitance values derived from C-V data for CAB binder and 1 M NaCl electrolyte. Similar trend is obtained with C-D data.

Another set of experiments was conducted with a PVA binder and larger amount of A-C (200 mg. Judging by the suspension color and sedimentation, the AuNP appeared to be aggregated and of larger size (~100 nm). Unlike the hydrophobic CAB, PVA is hydrophilic and better matches

with the water suspended AuNP as alluded to by [23]. PVA is less compatible with the hydrophobic current collector, made of grafoil. The electrolyte here was 1 M NaCl. Two sets of experiments were conducted and their averages are shown in Fig. 9 by the blue dots. The data are consistent up to 40  $\mu\text{g}/200\text{ mg}$  after which film homogeneity could become an issue.

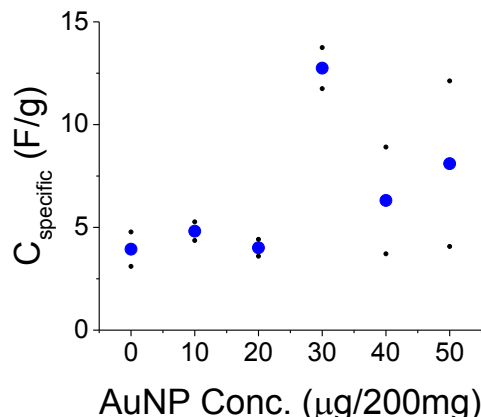


Figure 9. Specific capacitance values derived from C-V data for PVA binder and 1 M NaCl electrolyte. The black dots are the results from two sets of experiments; the blue dots are average of these two experiments.

### Simulations:

In the simulations, one compares two cases: (1) a cell without metal colloids; (2) a cell with colloids extruding into the neutral region. A portion of the S-C was modelled by a parallel plate capacitor with a graphitic film of finite conductance that is deposited on top of a metallic current collector. The gold particle is partially embedded inside the graphic film. The neutral region is situated at the cell's center and a bias is provided between the two current collectors:  $\pm V_{\text{in}}$ . The surface potential of the neutral region and the surface potential of the metal colloids are floating. The colloid radius was 10 nm. Larger particles would result in larger polarization effect, though experimentally, one would need to balance their size with the pore size of the A-C. The otherwise capacitance increase is diminished when the colloids are embedded away from the extended electrode. This corroborates the experiments; when the AuNP were mostly part of the electrolyte, the efficiency of the capacitor was substantially diminished. The conductivity of the graphitic material matters only if its conductance is comparable to the current collectors' value.

The potential distribution inside the cell with and without the metallic colloids is shown in Fig. 10. The local polarization is shown in Fig. 11. The latter points to polarization increase in the cell upon the presence of the AuNP.



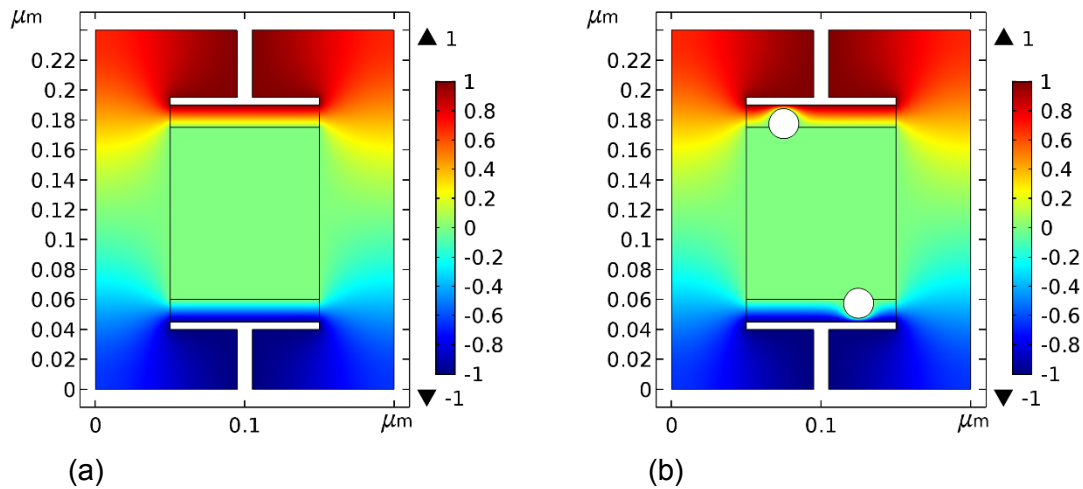


Figure 10. Potential distribution for  $V_{in}=1$  V. The neutral region indeed has a constant potential (zero in this case) and the presence of the metallic colloid alters the potential lines. (a) No colloid. (b) With 10 nm colloids. The thermal legend is in units of Volts.

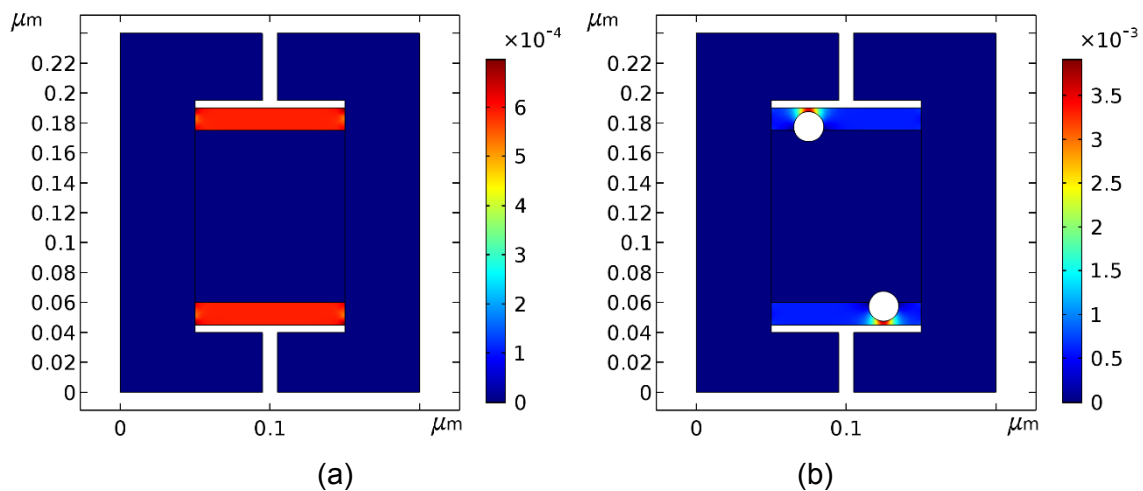


Figure 11. The absolute value of polarization is stronger near the colloids. The thermal legend is in units of  $C/m^3$ .

The capacitance of the cell is proportional to the charge on the electrode. Fig. 12 shows the change in the electrode charge as a function of the cell bias. The electrode charge,  $Q$ , is related to the bias,  $V_{in}$ , as,  $Q=C \cdot V_{in}$ , with  $C$ , the cell capacitance. The cell capacitance is therefore,  $C=Q/V_{in}$  and it is constant since the charge on the electrode varies linearly with  $V_{in}$ . The slope of the curve (the capacitance) increases upon presence of the AuNP. The curves of Fig. 12 are translated to cell capacitance values of: 0.133 and 0.22 nF, for respectively, cells without colloids and cells with them. Overall, one expects capacitance increase as a result of colloid presence.

While not shown, packing more colloids, say two AuNP on each surface, obviously increases the cell capacitance but up to a point. The cell capacitance for very closely packed colloids on each surface is actually smaller than when they are placed apart. Simulation wise, the change is not large (ca 2.5%), yet noticeable and is attributed to a dipole-dipole interaction.

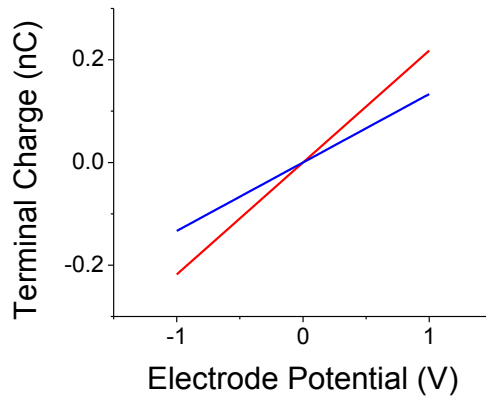


Figure 12. Change in electrode charge as a function of the bias,  $V_{in}$ . Blue line: no colloid; Red line: with colloids. The cell capacitance is the slope of the linear curve.

#### IV. Discussion

The surface science of gold colloids, embedded within a supercapacitor is complex. The colloids are coated with a negatively charged ligand, enabling it to attach to the active-carbon electrode but limiting its packing on the surface. The choice of particle size, the binder, the electrolyte and the porous material, matter. As with many surface science applications, the preparation of the sample is important too. Nevertheless, through experimentation and simulations we demonstrated an enhancement in the specific capacitance upon placing AuNP in the super capacitor cell and competing surface effects led to an optimum in its value.

#### V. Conclusion

Incorporating gold particles in aqueous, active-carbon-based supercapacitors exhibited a substantial enhancement in their specific capacitance values (both gravimetric and volumetric). Simulations point to a plasmonic effect by AuNP, when placed at the electrode/electrolyte interface.

## References:

1. Brown, John, and Willis Jackson. "The properties of artificial dielectrics at centimetre wavelengths." Proceedings of the IEE-Part B: Radio and Electronic Engineering 102.1 (1955): 11-16.
2. R. E. Collin, *Field Theory of Guided Waves*, Wiley-IEEE Press, 2nd edition, 1990.
3. Shih-Chang Wu and H Grebel, "Phase shifts in coplanar waveguides with patterned conductive top covers, J. Phys. D: Appl. Phys. 28 437-439 (1995)
4. H. Grebel and P. Chen, "Artificial dielectric polymeric waveguides: metallic embedded films ", JOSA A, 8, 615-618 (1991). <https://doi.org/10.1364/JOSAA.8.000615>
5. H. Grebel and P. Chen, "Artificial dielectric polymeric waveguides: semiconductor-embedded films", Opt. Letts, 15, 667-669 (1990). <https://doi.org/10.1364/OL.15.000667>
6. Keh-Chyun Tsay, Lei Zhang, JiuJun Zhang, *Electrochimica Acta* 60 (2012) 428–436.
7. Yudong Li, Xianzhu Xu, Yanzhen He, Yanqiu Jiang and Kaifeng Lin, *Polymers* 2017, 9, 2; doi:10.3390/polym9010002.
8. M. Kaempgen, C. K. Chan, J. Ma, Y. Cui, and G. Gruner, *Nano Letts.*, , 9 (2009) 1872.
9. Michio Inagaki, Hidetaka Konno, Osamu Tanaike, *Journal of Power Sources* 195 (2010) 7880–7903.
10. Zhang, S and Pan, N, 2015. DOI:10.1002/aenm.201401401. <https://escholarship.org/uc/item/26r5w8nc>
11. Mohammad S. Rahmanifar, Maryam Hemmati, Abolhassan Noori, Maher F. El-Kady, Mir F. Mousavi, Richard B. Kaner, *Materials Today Energy* 12 (2019) 26-36. <https://doi.org/10.1016/j.mtener.2018.12.006>
12. Xin Miao, Roberto Rojas-Cessa, Ahmed Mohamed and Haim Grebel, *IEEE IoT*, 2018
13. Roberto Rojas-Cessa, Haim Grebel, Zhengqi Jiang, Camila Fukuda, Henrique Pita, Tazima S. Chowdhury, Ziqian Dong and Yu Wan, *Environmental Progress & Sustainable Energy*, 37, (2018) 155-164. DOI 10.1002/ep.
14. Emre O. Polat and Coskun Kocabas, *Nano Lett.* 2013, 13, 5851–5857. [dx.doi.org/10.1021/nl402616t](https://doi.org/10.1021/nl402616t).
15. John Turkevich, "Colloidal Gold. Part I: HISTORICAL AND PREPARATIVE ASPECTS, MORPHOLOGY AND STRUCTURE", *Gold Bull.*, 1985, 18, 86-91.
16. John Turkevich, " Colloidal Gold. Part II: COLOUR, COAGULATION, ADHESION, ALLOYING AND CATALYTIC PROPERTIES", *Gold Bull.*, 1985, 18, 125-131.
17. Mercado-Lubo, R.; Zhang, Y.; Zhao, L.; Rossi, K.; Wu, X.; Zou, Y.; Castillo, A.; Leonard, J.; Bortell, R.; Greiner, D. L.; Shultz, L. D.; Han, G.; McCormick, B. A. *Nature Communications* 2016, 12225.
18. H. Grebel, " Asymmetric Supercapacitors: Optical and Thermal Effects When Active Carbon Electrodes Are Embedded with Nano-Scale Semiconductor Dots", *C* 2021, 7(1), 7; <https://doi.org/10.3390/c70100072> .
19. H. Grebel, "Optically Controlled Supercapacitors: Functional Active Carbon Electrodes with Semiconductor Particles", *Materials* 2021, 14(15), 4183; <https://doi.org/10.3390/ma14154183>

20. Bing-Ang Mei, Obaidallah Munteshari, Jonathan Lau, Bruce Dunn, and Laurent Pilon, "Physical Interpretations of Nyquist Plots for EDLC Electrodes and Devices", *J. Phys. Chem. C* 2018, 122, 194–206. DOI: 10.1021/acs.jpcc.7b10582.
21. Y. Gogotsi and P. Simon, "True Performance Metrics in Electrochemical Energy Storage", *Science* 334, 917 (2011). DOI: 10.1126/science.1213003
22. Suvi Lehtimäki, Anna Railanmaa, Jari Keskinen, Manu Kujala, Sampo Tuukkanen Donald Lupo, "Performance, stability and operation voltage optimization of screen-printed aqueous supercapacitors", *Scientific Reports*, 7:46001 (2017). DOI: 10.1038/srep46001
23. Qinxing Xie, Xiaolin Huang, Yufeng Zhang, Shihua Wu, Peng Zhao, "High performance aqueous symmetric supercapacitors based on advanced carbon electrodes and hydrophilic poly(vinylidene fluoride) porous separator", *Applied Surface Science* 443 (2018) 412–420.